

Electroweak baryogenesis and electron EDM in the B-LSSM

Jin-Lei Yang^{1,2,3*}, Tai-Fu Feng^{1,2,4†}, Hai-Bin Zhang^{1,2‡}

Department of Physics, Hebei University, Baoding, 071002, China¹

Hebei Key Lab of High-precision Computation and Application

of Quantum Field Theory, Baoding, 071002, China²

CAS Key Laboratory of Theoretical Physics, School of Physical Sciences,

University of Chinese Academy of Sciences, Beijing 100049, China³

Department of Physics, Chongqing University, Chongqing 401331, China⁴

Abstract

Electroweak baryogenesis (EWB) and electric dipole moment (EDM) have close relation with the new physics beyond the standard model (SM), because the SM CP-violating (CPV) interactions are not sufficient to provide the baryon asymmetry of the universe by many orders of magnitude, and the theoretical predictions for the EDM of electron (d_e) in the SM are too tiny to be detected in near future. In this work, we explore the CPV effects on EWB and the electron EDM in the minimal supersymmetric extension (MSSM) of the SM with local $B - L$ gauge symmetry (B-LSSM). And the two-step transition via tree-effects in this model is discussed. Including two-loop corrections to d_e and considering the constrains from updated experimental data, the numerical results show that the B-LSSM can account for the observed baryon asymmetry. In addition, when the cancellation between different contributions to d_e takes place, the region favored by EWB can be compatible with the corresponding EDM bound.

PACS numbers:

Keywords: EWB, EDM, B-LSSM

* yangjinlei@itp.ac.cn

† fengtf@hbu.edu.cn

‡ hzbzhang@hbu.edu.cn

I. INTRODUCTION

Despite the considerable success of the Standard Model (SM) in describing a large amount of experimental observations, there are still various evidences beyond the SM. One of the most interesting problems is the baryon asymmetry of the universe (BAU) [1, 2]:

$$Y_B \equiv \frac{\rho_B}{s} = \begin{cases} (8.2 - 9.4) \times 10^{-11} & (95\% \text{CL}), \text{ Big Bang Nucleosynthesis} \\ 8.65 \pm 0.09 \times 10^{-11}, & \text{PLANCK} \end{cases} \quad (1)$$

where ρ_B is the baryon number density, s is the entropy density of the universe. The SM CP-violating (CPV) interactions are not sufficient to provide the asymmetry by many orders of magnitude, which indicates that the SM is incomplete. The search for new physics (NP) beyond the SM is motivated in part by the desire to overcome the failure of the SM to explain the BAU. Electroweak baryogenesis (EWB) [3] is an explanation of the origin of the cosmological asymmetry between matter and antimatter, and new CPV terms are needed to enhance the asymmetry theoretically.

Meanwhile, new CPV phases can provide much larger values of the electric dipole moments (EDMs) than the SM predictions. The SM prediction for the electron EDM is about $10^{-38} \text{e} \cdot \text{cm}$ [4–6], which is impossible to be detected by present experiments. However, when new CPV phases are introduced, the enhanced electron EDM may be detected in near future, which can be regarded as a smoking gun for NP beyond the SM. The upper bounds on d_e have been obtained [7–9]

$$|d_e| < 8.7 \times 10^{-29} \text{e} \cdot \text{cm}. \quad (2)$$

Since the experimental upper bound on the electron EDM is very small, the contributions from new CPV phases are limited strictly by the present experimental data, and researching NP effects on the electron EDM may shed light on the mechanism of CPV.

In extensions of the SM, the supersymmetry is considered as one of the most plausible candidates. And the analysis of EWB in the minimal supersymmetric extension of the SM (MSSM) are discussed in detail in Refs. [10–22], and in nonminimal supersymmetric models are discussed in Refs. [23–27], which indicates that the main contributions to Y_B come from the T -terms (the trilinear scalar terms in the soft supersymmetry breaking potential) and

the μ term (the bilinear Higgs mass term in the superpotential). The supersymmetric effects on the EDM of electron has been explored in Refs. [28–40]. The results show that the most interesting possibility to suppress the electron EDM to below the corresponding experimental upper bound is, the contributions from different phases cancel each other. However, if we assume that the only CPV phases come from μ and T , the value of them is limited strictly by the experimental upper bounds on d_e . In a word, the CPV characters in supersymmetry are very interesting and studies on them may shed some light on the general characteristics of the supersymmetric model.

The MSSM with local $B - L$ gauge symmetry (B-LSSM) [41–44] is based on the gauge symmetry group $SU(3) \otimes SU(2)_L \otimes U(1)_Y \otimes U(1)_{B-L}$, where B stands for the baryon number and L stand for the lepton number respectively. Compared with the MSSM, B-LSSM can provide much more candidates for the dark matter [45–48], and the invariance under $U(1)_{B-L}$ gauge group imposes the R-parity conservation which is assumed in the MSSM to avoid proton decay. In addition, the model also alleviates the little hierarchy problem of the MSSM [49–55]. In this paper, we explore the CPV effects on Y_B and the electron EDM d_e in the B-LSSM. And the possible cancellation between different contributions to d_e is explored, which is different from the case in the MSSM. Compared with the MSSM, there are new CPV terms in the B-LSSM, the cancellation between the contributions to d_e from these new CPV phases and the phase of M_1 which is the phase of gaugino mass term, in this paper. Moreover, there are two mass terms which can be small and make contributions to d_e , the effects of them are also explored in detail.

The paper is organized as follows. In Sec.II, we describe the B-LSSM briefly by introducing the superpotential and the general soft breaking terms. Then the analysis on electroweak phase transition (PT), Y_B and the electron EDM d_e in the B-LSSM are presented in Sec.III. In Sec.IV, we explore the CPV effects on Y_B , d_e by varying different parameters. Conclusions are summarized in Sec.V.

II. THE B-LSSM

In the B-LSSM, two chiral singlet superfields $\hat{\eta}_1 \sim (1, 1, 0, -1)$, $\hat{\eta}_2 \sim (1, 1, 0, 1)$ and three generations of right-handed neutrinos are introduced, which allow for a spontaneously broken $U(1)_{B-L}$ without necessarily breaking R-parity. In addition, this version of B-LSSM is encoded in SARAH [56], which is used to create the mass matrices and interaction vertexes in the model. Meanwhile, the superpotential of the B-LSSM can be written as

$$W = Y_u^{ij} \hat{Q}_i \hat{H}_2 \hat{U}_j^c + \mu \hat{H}_1 \hat{H}_2 - Y_d^{ij} \hat{Q}_i \hat{H}_1 \hat{D}_j^c - Y_e^{ij} \hat{L}_i \hat{H}_1 \hat{E}_j^c + Y_{\nu, ij} \hat{L}_i \hat{H}_2 \hat{\nu}_j^c - \mu' \hat{\eta}_1 \hat{\eta}_2 + Y_{x, ij} \hat{\nu}_i^c \hat{\eta}_1 \hat{\nu}_j^c, \quad (3)$$

where i, j are generation indices. Then the soft breaking terms of the B-LSSM are generally given as

$$\begin{aligned} \mathcal{L}_{soft} = & \left[-\frac{1}{2}(M_1 \tilde{\lambda}_B \tilde{\lambda}_B + M_2 \tilde{\lambda}_W \tilde{\lambda}_W + M_3 \tilde{\lambda}_g \tilde{\lambda}_g + 2M_{BB'} \tilde{\lambda}_{B'} \tilde{\lambda}_B + M_{B'} \tilde{\lambda}_{B'} \tilde{\lambda}_{B'}) - \right. \\ & B_\mu H_1 H_2 - B_{\mu'} \tilde{\eta}_1 \tilde{\eta}_2 + T_{u, ij} \tilde{Q}_i \tilde{u}_j^c H_2 + T_{d, ij} \tilde{Q}_i \tilde{d}_j^c H_1 + T_{e, ij} \tilde{L}_i \tilde{e}_j^c H_1 + T_\nu^{ij} H_2 \tilde{\nu}_i^c \tilde{L}_j + \\ & T_x^{ij} \tilde{\eta}_1 \tilde{\nu}_i^c \tilde{\nu}_j^c + h.c. \left. \right] - m_{\tilde{\nu}, ij}^2 (\tilde{\nu}_i^c)^* \tilde{\nu}_j^c - m_{\tilde{q}, ij}^2 \tilde{Q}_i^* \tilde{Q}_j - m_{\tilde{u}, ij}^2 (\tilde{u}_i^c)^* \tilde{u}_j^c - m_{\tilde{\eta}_1}^2 |\tilde{\eta}_1|^2 - \\ & m_{\tilde{\eta}_2}^2 |\tilde{\eta}_2|^2 - m_{\tilde{d}, ij}^2 (\tilde{d}_i^c)^* \tilde{d}_j^c - m_{\tilde{L}, ij}^2 \tilde{L}_i^* \tilde{L}_j - m_{\tilde{e}, ij}^2 (\tilde{e}_i^c)^* \tilde{e}_j^c - m_{H_1}^2 |H_1|^2 - m_{H_2}^2 |H_2|^2, \quad (4) \end{aligned}$$

where $\tilde{\lambda}_B, \tilde{\lambda}_{B'}$ denoting the gaugino of $U(1)_Y$ and $U(1)_{(B-L)}$ respectively. The local gauge symmetry $SU(2)_L \otimes U(1)_Y \otimes U(1)_{B-L}$ breaks down to the electromagnetic symmetry $U(1)_{em}$ as the Higgs fields receive vacuum expectation values (VEVs):

$$\begin{aligned} H_1^1 &= \frac{1}{\sqrt{2}}(v_1 + \text{Re}H_1^1 + i\text{Im}H_1^1), & H_2^2 &= \frac{1}{\sqrt{2}}(v_2 + \text{Re}H_2^2 + i\text{Im}H_2^2), \\ \tilde{\eta}_1 &= \frac{1}{\sqrt{2}}(u_1 + \text{Re}\tilde{\eta}_1 + i\text{Im}\tilde{\eta}_1), & \tilde{\eta}_2 &= \frac{1}{\sqrt{2}}(u_2 + i\text{Re}\tilde{\eta}_2 + i\text{Im}\tilde{\eta}_2). \end{aligned} \quad (5)$$

For convenience, we define $u^2 = u_1^2 + u_2^2$, $v^2 = v_1^2 + v_2^2$ and $\tan \beta' = \frac{u_2}{u_1}$ in analogy to the ratio of the MSSM VEVs ($\tan \beta = \frac{v_2}{v_1}$).

New $U(1)_{B-L}$ gauge group introduces new gauge boson Z' and the corresponding gauge coupling constant g_B . In addition, two Abelian groups gives rise to a new effect absent in the MSSM or other SUSY models with just one Abelian gauge group: the gauge kinetic mixing. Immediate interesting consequence of the gauge kinetic mixing arise in various sectors of the

model. Firstly, new gauge boson Z' mixes with the Z boson in the MSSM, and new gauge coupling constant g_{YB} is introduced. Then the gauge kinetic mixing leads to the mixing between the H_1^1 , H_2^2 , $\tilde{\eta}_1$, $\tilde{\eta}_2$ at the tree level, and $\tilde{\lambda}_{B'}$ mixes with the two higgsinos in the MSSM at the tree level. Meanwhile, additional D-terms contribute to the mass matrices of the squarks and sleptons. All of these properties affect the theoretical predictions for Y_B and d_e in the B-LSSM, and the model are introduced in detail in our earlier work [57–59].

III. EWB AND ELECTRON EDM IN THE B-LSSM

A. Electroweak phase transition

In the MSSM, EWB has been excluded because the strong first order PT with very light right handed stop $< 120\text{GeV}$ is not possible after the discovery of the 125 GeV Higgs boson [60–69]. With respect to the MSSM, a strong two-step PT can be achieved in the B-LSSM, because there are two additional scalar singlets. These new singlets mix with the two doublets in the MSSM at the tree level through gauge kinetic mixing, which change the effective potential vastly. For simplicity, the temperature dependence of β , β' is neglected and the tree-level effective potential can be written as

$$V_{eff}(h, \eta) = \frac{1}{2}M(T)^2 h^2 + \frac{1}{2}m_\eta^2 \eta^2 + \frac{1}{32}(g_1^2 + g_2^2 + g_{YB}^2)c_{2\beta}^2 h^4 + \frac{1}{8}g_B^2 c_{2\beta'}^2 \eta^4 + \frac{1}{8}g_B g_{YB} c_{2\beta} c_{2\beta'} h^2 \eta^2, \quad (6)$$

where

$$M(T)^2 \equiv M_0^2 + \mathcal{G}T^2 = m_{H_1}^2 c_\beta^2 + m_{H_2}^2 s_\beta^2 + 2\mu^2 - B_\mu s_{2\beta} + \mathcal{G}T^2, \quad (7)$$

$$m_\eta^2 = m_{\eta_1}^2 c_{\beta'}^2 + m_{\eta_2}^2 s_{\beta'}^2 + 2\mu_\eta^2 - B_\eta s_{2\beta'}, \quad (8)$$

$$c_\beta \equiv \cos \beta, \quad s_\beta \equiv \sin \beta, \quad c_{2\beta} \equiv \cos 2\beta, \quad s_{2\beta} \equiv \sin 2\beta, \quad (9)$$

and T denotes temperature, \mathcal{G} is the sum of relevant couplings, h and η acquire VEVs $\langle h \rangle = v$, $\langle \eta \rangle = u$ respectively at zero temperature (present universe). Since the singlets couples to fewer degrees of freedom, their thermal masses is lower than that of the SM higgs, and we ignore their thermal mass. At very high temperature, h and η are stabilized at the

origin. In addition, it can be noted in Eq. (6, 7) that, the only possible gauge-dependence term is $\mathcal{G}T^2$, and the gauge-independence of $\mathcal{O}(T^2)$ term was proved in the appendix C of Ref. [70]. Hence our analysis of the electroweak PT is gauge invariant. As the universe cools, the singlets transition to a nonzero VEV u_{c1} first, in a second order phase transition at T_{c1} . Then at temperature $T_{c2} \sim m_W < T_{c1}$, the universe undergoes a first order PT to (v_{c2}, u) . Then we can obtain v_{c2} and $M(T)^2$ by solving the equations

$$\begin{cases} V_{eff}(0, u_{c1}) \Big|^{T_{c1}} = V_{eff}(v_{c2}, u) \Big|^{T_{c2}}, \\ \frac{\partial V_{eff}}{\partial h} \Big|_{(v_{c2}, u)}^{T_{c2}} = 0. \end{cases} \quad (10)$$

Then the first order transition temperature T_{c2} can be obtained by $\sqrt{(M(T)^2 - M_0^2)/\mathcal{G}}$. For the EWB to work, the sphaleron process must be decoupled when the electroweak PT completes. In other words, the sphaleron rate in the broken phase should be less than the Hubble parameter at that moment. In general, the sphaleron decoupling condition is cast into the form $v_{c2}/T_{c2} \gtrsim 1$. And in our chosen parameter space in the next section, we have $v_{c2}/T_{c2} \gtrsim 1.5$, which is sufficient for the taking place of EWB.

B. Baryon asymmetry Y_B

The CPV effects enter as source terms in the quantum transport equations that govern the production of chiral charge at the phase boundary. According to Ref. [14], a simple expression for the baryon-to-entropy ratio can be written as

$$Y_B = -F_1 \sin \theta_\mu + F_2 \sin(-\theta_\mu + \theta_T). \quad (11)$$

where we have taken the gaugino mass terms $M_{1,2,B'}$ to be real, θ_μ , θ_T are the phases of μ and T_e respectively. Compared with the expression in Ref. [14], the additional minus sign on θ_μ comes from different definition of μ . The coefficients F_i depend on the mass parameters in the B-LSSM, such as μ , M_1 , M_2 , $M_{B'}$, A_0 (we assume that T-terms are all same at the GUT scale, $T_u/Y_u = T_d/Y_d = T_e/Y_e = A_0$, where $Y_{u,d,e}$ are the corresponding Yukawa coupling constants) and squark masses $M_{\tilde{t}_L}$, $M_{\tilde{t}_R}$. In addition, F_i also have a overall dependence

on bubble wall parameters v_w , L_w , $\Delta\beta$. For the concrete expressions of F_i , we adopt the formulas displayed in Ref. [14]. Compared with the MSSM, there is new contribution to $S_{\tilde{H}}^{CP}$ (the CPV higgsino source) in the B-LSSM, which comes from the mixing between new gaugino $\tilde{\lambda}_{B'}$ and the two higgsinos in the MSSM through gauge kinetic mixing, and the corresponding gauge coupling constant is g_{YB} .

C. The EDM of electron d_e

The effective Lagrangian for the electron EDM can be written as

$$\mathcal{L}_{EDM} = -\frac{i}{2}d_e\bar{l}_e\sigma^{\mu\nu}\gamma_5 l_e F_{\mu\nu}. \quad (12)$$

where $\sigma^{\mu\nu} = i[\gamma^\mu, \gamma^\nu]/2$, and $F_{\mu\nu}$ is the electromagnetic field strength. Adopting the effective Lagrangian approach, we can get

$$d_e = -\frac{2eQ_fm_e}{(4\pi)^2}\Im(C_2^R + C_2^{L*} + C_6^R), \quad (13)$$

where $Q_f = -1$, m_e denotes the electron mass, and $C_{2,6}^{L,R}$ represent the Wilson coefficients of the corresponding operators $O_{2,6}^{L,R}$

$$\begin{aligned} O_2^{L,R} &= \frac{eQ_f}{(4\pi)^2}(-iD_\alpha^*)\bar{l}_e\gamma^\alpha F \cdot \sigma P_{L,R}l_e, \\ O_6^{L,R} &= \frac{eQ_fm_e}{(4\pi)^2}\bar{l}_e F \cdot \sigma P_{L,R}l_e, \end{aligned} \quad (14)$$

where $D_\alpha = \partial_\alpha + iA_\alpha$, l_e is the wave function for electron, and $P_{R,L} = (1 \pm \gamma_5)/2$. Then, the Feynman diagrams contributing to the above Wilson coefficients are depicted by Fig. 1. Calculating the Feynman diagrams, the electron EDM can be written as

$$\begin{aligned} d_e^{(1)} &= \frac{-2}{em_e}\Im\left\{x_e[-I_3(x_{F_j}, x_{S_i}) + I_4(x_{F_j}, x_{S_i})][(C_{\tilde{l}_e S_i F_j}^L C_{\tilde{F}_j S_i l_e}^R) + (C_{\tilde{l}_e S_i F_j}^R C_{\tilde{F}_j S_i l_e}^L)^*]\right. \\ &\quad \left.+ \sqrt{x_e x_{F_j}}[-2I_1(x_{F_j}, x_{S_i}) + 2I_3(x_{F_j}, x_{S_i})]C_{\tilde{l}_e S_i F_j}^R C_{\tilde{F}_j S_i l_e}^R\right\}, \\ d_e^{(2)} &= \frac{-2}{em_e}\Im\left\{x_e[-I_1(x_{F_j}, x_{S_i}) + 2I_3(x_{F_j}, x_{S_i}) - I_4(x_{F_j}, x_{S_i})][(C_{\tilde{l}_e S_i F_j}^R C_{\tilde{F}_j S_i l_e}^L) \right. \\ &\quad \left.+ (C_{\tilde{l}_e S_i F_j}^L C_{\tilde{F}_j S_i l_e}^R)^*] + \sqrt{x_e x_{F_j}}[2I_1(x_{F_j}, x_{S_i}) - 2I_2(x_{F_j}, x_{S_i}) - 2I_3(x_{F_j}, x_{S_i})]\right. \\ &\quad \left.\times C_{\tilde{l}_e S_i F_j}^R C_{\tilde{F}_j S_i l_e}^R\right\}, \end{aligned} \quad (15)$$

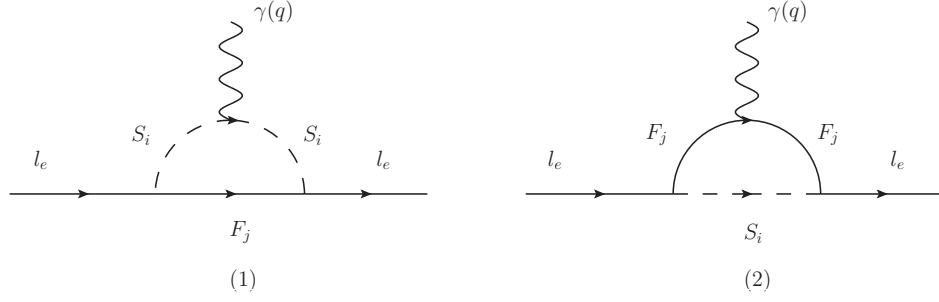


FIG. 1: The one-loop level diagrams contribute to the electron EDM, where (a) represents the charged scalars loops, and (b) represents the charged fermions loops.

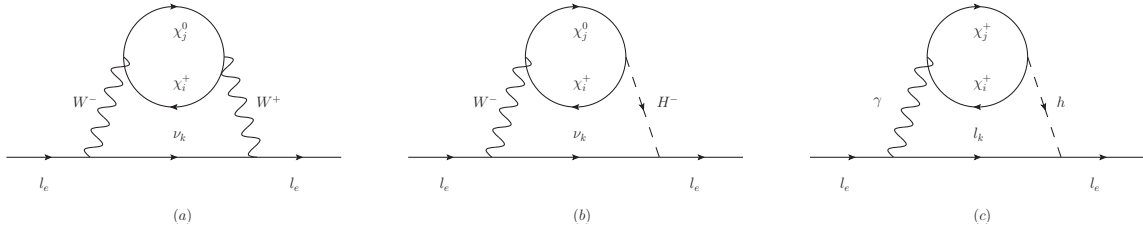


FIG. 2: The two-loop Barr-Zee type diagrams in which a closed fermion loop is attached to the virtual gauge bosons or Higgs fields, the corresponding contributions to d_e are obtained by attaching a photon to the internal particles in all possible ways.

where $x_i = m_i^2/m_W^2$, $C_{abc}^{L,R}$ denotes the constant parts of the interactional vertex about abc , which can be got through SARAH, a, b, c denote the interactional particles, and the concrete expressions for the functions $I_{1,2,3,4}$ can be found in [71, 72]. In addition, our earlier work [59] shows that, two-loop Barr-Zee type diagrams can make important contributions to the muon magnetic dipole moment (MDM), and we consider the contributions from the two-loop diagrams in which a closed fermion loop is attached to the virtual gauge bosons or Higgs fields. According to Ref. [73], the main two-loop diagrams contributing to the electron EDM are shown in Fig. 2. Assuming $m_F = m_{\chi_i^+} = m_{\chi_j^0} \gg m_W$, $m_F = m_{\chi_i^+} \gg m_h$, the contributions from the two-loop diagrams to d_e can be simplify as

$$d_e^{(a)} = \frac{3G_F m_W \sqrt{x_e}}{-64\sqrt{2}\pi^4} \left\{ \Im(C_{f_j W f_i}^L C_{f_j W f_i}^{R*}) \right\},$$

$$d_e^{(b)} = \frac{G_F e m_W C_{l_e H \nu_k}^L}{256\pi^4 g_2 \sqrt{x_F}} \left\{ \left[179/36 + 10/3 J(x_F, x_W, x_H) \right] \Im(C_{f_i H f_j}^L C_{f_j W f_i}^L + C_{f_i H f_j}^R C_{f_j W \chi_i^+}^R) \right\}$$

$$\begin{aligned}
& + \left[-1/9 - 2/3 J(x_F, x_W, x_H) \right] \Im(C_{\tilde{f}_i H f_j}^L C_{\tilde{f}_j W f_i}^R + C_{\tilde{f}_i H f_j}^R C_{\tilde{f}_j W f_i}^L) \\
& + \left[-16/9 - 8/3 J(x_F, x_W, x_H) \right] \Im(C_{\tilde{f}_i H f_j}^L C_{\tilde{f}_j W f_i}^L - C_{\tilde{f}_i H f_j}^R C_{\tilde{f}_j W \chi_i^+}^R) \\
& + \left[-2/9 - 4/3 J(x_F, x_W, x_H) \right] \Im(C_{\tilde{f}_i H f_j}^L C_{\tilde{f}_j W f_i}^R - C_{\tilde{f}_i H f_j}^R C_{\tilde{f}_j W f_i}^L), \\
d_e^{(c)} = & \frac{G_F e m_W C_{\tilde{l}_e h^0 l_e}}{64 \pi^4 \sqrt{x_F}} \Im(C_{\tilde{f}_i h^0 f_i}^L) \left[1 + \ln \frac{x_F}{x_h} \right], \tag{16}
\end{aligned}$$

where f_j, f_i denote χ_j^0 and χ_i^\pm respectively, W denotes W boson, H denotes charged Higgs boson, h denotes SM-like Higgs boson, the concrete expressions for the function J can be found in Ref. [59].

Compared with the MSSM, there are new CPV terms $M_{BB'}$, $M_{B'}$ and μ' can contribute to the electron EDM. In the next section, we will explore the possible cancellation between the contributions to d_e from these new CPV terms and M_1 . Moreover, it is more interesting that there are two new mass terms in the B-LSSM, the mixing mass term $M_{BB'}$ between $\tilde{\lambda}_B$, $\tilde{\lambda}_{B'}$, and $M_{B'}$ which is the mass term of $\tilde{\lambda}_{B'}$. Both of $M_{BB'}$ and $M_{B'}$ can be very small and the gaugino masses still can be large enough to satisfy the experimental upper bounds on gaugino masses. The contributions to the electron EDM from the phases of $M_{BB'}$ or $M_{B'}$ can be highly suppressed by small $M_{BB'}$ or $M_{B'}$ to satisfy the present experimental upper bound on d_e .

IV. NUMERICAL ANALYSES

In this section, we present the numerical results of Y_B and electron EDM d_e in the B-LSSM. The EDMs of neutron, mercury, heavy quarks are discussed in our previous work [74], and some two-loop Barr-Zee and gluino type corrections are considered, the numerical results show that the constraints from these quantities are less strict than the constraints from the electron EDM. Hence, the allowed regions by the present upper limit on d_e can coincide with the upper limits on EDMs of neutron, mercury and heavy quarks. The relevant SM input parameters are chosen as $m_W = 80.385$ GeV, $m_Z = 90.1876$ GeV, $\alpha_{em}(m_Z) = 1/128.9$, $\alpha_s(m_Z) = 0.118$. We take $Y_\nu = Y_x = 0$ approximately due to the tiny neutrino masses basically do not affect the numerical analysis. The SM-like Higgs boson mass is 125.18 GeV [8] and constrains the parameter space strictly. Compared with the MSSM,

new singlets mix with the MSSM doublets at the tree level in the B-LSSM, which can affect the theoretical prediction of SM-like Higgs mass. Including the leading-log radiative corrections from stop and top particles [75–77], the lightest Higgs mass in the B-LSSM is limited in the range $124 \text{ GeV} < m_h < 126 \text{ GeV}$ in our chosen parameter space below.

The updated experimental data [78] on searching Z' indicates $M_{Z'} \geq 4.05 \text{ TeV}$ at 95% Confidence Level (CL). And an upper bound on the ratio between the Z' mass and its gauge coupling is given in Refs. [79, 80] at 99% CL as $M_{Z'}/g_B > 6 \text{ TeV}$. In our earlier work [59], we explore the effects of parameters $\tan \beta$, $\tan \beta'$, g_B , g_{Y_B} and slepton masses $M_{\tilde{L}, \tilde{e}}$ on the muon MDM in the B-LSSM without CPV. Since the CPV phases affect the electron EDM more obviously than the muon MDM, we explore the CPV effects on the electron EDM firstly in this paper, but put off the exploration of CPV effects on the muon MDM in our next work. Then considering the experimental data of the muon MDM, we choose $M_{Z'} = 4.2 \text{ TeV}$, $\tan \beta = 10$, $\tan \beta' = 1.15$, $g_B = 0.4$, $M_{\tilde{L}, \tilde{e}} = \text{diag}(2, 2, 2) \text{ TeV}$. We don't fix g_{Y_B} because it affects the numerical result of Y_B obviously through the contributions from new gaugino $\tilde{\lambda}_{B'}$. Considering the constraints from the experiments [8], for those parameters in higgsino and gaugino sectors, we appropriately fix $M_1 = \frac{1}{2}M_2 = \frac{1}{2}M_{B'} = \frac{1}{2}M_{BB'} = 0.3 \text{ TeV}$, $\mu' = 0.8 \text{ TeV}$ for simplicity. The value of μ is not fixed, because the main contributions to Y_B come from the μ term. In addition, in order to satisfy the experimental data on $\bar{B} \rightarrow X_s \gamma$ and $B_s^0 \rightarrow \mu^+ \mu^-$ [58], we take the stop mass $m_{\tilde{t}_L} = m_{\tilde{t}_R} = 1.5 \text{ TeV}$, charged Higgs boson mass $M_{H^\pm} = 1.5 \text{ TeV}$ for simplicity. According to Refs. [81–83], the size of the scalar trilinear couplings are limited by the conditions of avoiding charge and color breaking minima, then we can take $A_0 = 0.1 \text{ TeV}$, which can satisfy this condition. For the bubble wall parameters v_w , L_w , we adopt the central values $v_w = 0.05$, $L_w = 25/T$ [84, 85], and $\Delta\beta$ as a function of pseudoscalar Higgs boson mass provided in Ref. [84], we take $\Delta\beta = 0.015$. For the thermal widths, we adopt the results in Ref. [86] in the following analysis.

In order to see how θ_μ , θ_{A_0} and μ affect Y_B , we take $g_{Y_B} = -0.4$ and scan the regions of the parameter space [$\theta_\mu = (-\pi, \pi)$, $\theta_{A_0} = (-\pi, \pi)$, $\mu = (0.1, 1) \text{ TeV}$]. In the scanning, we keep Y_B in the region $(8.2 - 9.4) \times 10^{-11}$. Then the allowed region of θ_μ and μ is displayed in Fig. 3. From the picture, we can see that there are two ellipses in the figure, and the two ellipses mainly concentrate on the vicinity of $\mu = 600 \text{ GeV}$ and $\mu = 300 \text{ GeV}$ respectively,

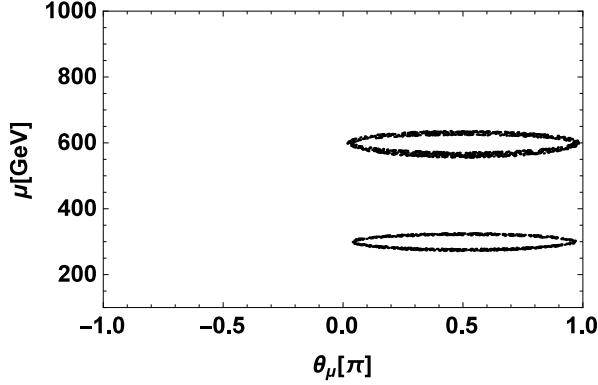


FIG. 3: Keeping Y_B in the region $(8.2 - 9.4) \times 10^{-11}$, the allowed region of θ_μ and μ .

because the effects of these interactions are resonantly enhanced when μ is comparable to the mass terms $M_{1,2,B'}$ [87, 88], the observed baryon asymmetry can be accounted for only in this case. The allowed region of θ_μ is concentrated on $\theta_\mu > 0$, because the mainly contributions come from the coefficient F_1 , and F_1 is negative in our chosen parameter space. In addition, with the increasing of θ_μ , the value of μ has a small deviation from $M_{1,B'}$ or M_2 , because the contributions to Y_B with large θ_μ will exceed 9.4×10^{-11} when μ equals to $M_{1,B'}$ or M_2 . It also can be noted from picture that, the minimum value of θ_μ is about 0.03 for $\mu = 600$ GeV, 0.04 for $\mu = 300$ GeV, and there are more points in the vicinity of $\mu = 600$ GeV. In our chosen parameter space, the value of $M_{B'}$ is 600 GeV, and there is also a resonant enhancement when $\mu = M_{B'}$. Hence, there are more points in the vicinity of $\mu = 600$ GeV and the minimum value of θ_μ is smaller slightly for $\mu = 600$ GeV than $\mu = 300$ GeV.

Then we take $\theta_\mu = 0.03$, $\mu = 600$ GeV, and explore how θ_{A_0} and new parameter g_{YB} affect the numerical result. Y_B versus θ_{A_0} for $g_{YB} = -0.3$ (solid line), -0.4 (dashed line), -0.5 (dotted line) is plotted in Fig. 4, where the gray area denotes the experimental interval $(8.2 - 9.4) \times 10^{-11}$. Compared with the MSSM, new parameter g_{YB} can affect the numerical result obviously, and Y_B increases with the increasing of $|g_{YB}|$, because the contribution from new gaugino $\tilde{\lambda}_{B'}$ is proportional to g_{YB}^2 [14]. From the picture we can see that, in our chosen parameter space, the allowed region of θ_{A_0} is larger when $g_{YB} = -0.4$ than $g_{YB} = -0.3$ or -0.5 . The value of g_{YB} under which the allowed region of θ_{A_0} is largest depends on the value

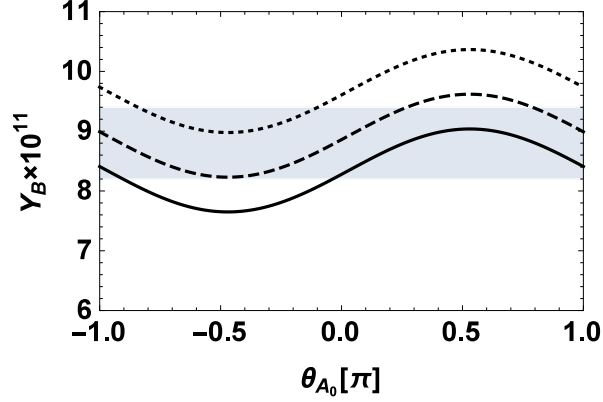


FIG. 4: Y_B versus θ_{A_0} for $g_{YB} = -0.3$ (solid line), -0.4 (dashed line), -0.5 (dotted line), and the gray area denotes the experimental interval $(8.2 - 9.4) \times 10^{-11}$.

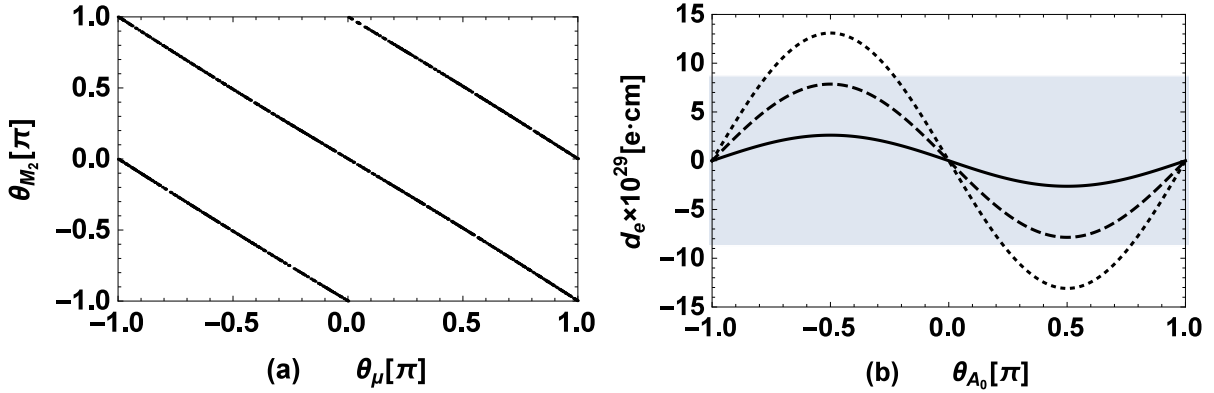


FIG. 5: Keeping $|d_e| < 8.7 \times 10^{-29}$, the cancellation between θ_{M_2} and θ_μ (a) are shown. And d_e versus θ_{A_0} are plotted for $A_0 = 0.1$ TeV (solid line), 0.3 TeV (dashed line), 0.5 TeV (dotted line), where the gray area denotes the present experimental upper bound on d_e .

of θ_μ and μ , because the main contributions to Y_B come from the μ term.

From the numerical results of Y_B , we can see that the minimum value of θ_μ is about 0.03 when EWB can take place. However, in this case, the contributions to the electron EDM d_e are enhanced vastly, and d_e exceeds the corresponding upper bound by several orders of magnitude. Hence, the contributions from different CPV phases should cancel each other to satisfy the present experimental upper bound. Then we take $g_{YB} = -0.4$, and explore the cancellation between θ_{M_2} and θ_μ by taking other CPV phases equal to 0 . We scan the

regions of the parameter space $[\theta_{M_2} = (-\pi, \pi), \theta_\mu = (-\pi, \pi)]$, and keep $|d_e| < 8.7 \times 10^{-29}$ in the scanning. The numerical results are shown in Fig. 5 (a). In addition, θ_{A_0} can also make important contributions to Y_B , hence it is interesting to explore how θ_{A_0} affects d_e . Since the effects of θ_{A_0} are highly suppressed by small Y_e , we do not have to cancel the contributions from θ_{A_0} to d_e . Then we plot d_e versus θ_{A_0} in Fig. 5 (b), where the gray area denotes the experimental upper bound on d_e , the solid, dashed and dotted lines denote $A_0 = 0.1$ TeV, 0.3 TeV, 0.5 TeV, respectively.

From the pictures we can see that, the contributions from θ_{M_2} and θ_μ are cancelled when $\theta_{M_2} \approx -\theta_\mu + n\pi$ ($n = 0, \pm 1$), the phases we chosen to cancel each other due to that, the contributions from θ_{M_2} and θ_μ are comparable. In addition, the contributions from θ_{A_0} are enlarged by large A_0 , and the contributions from θ_{M_2} , θ_μ are larger than θ_{A_0} by several orders of magnitude, hence the contributions from θ_μ are hardly cancelled by θ_{A_0} (when the cancellation between θ_μ and θ_{A_0} takes place, the maximum value of θ_μ is $\mathcal{O}(10^{-3})$, which is not sufficient for the taking place of EWB). It is different from the case in the MSSM [38], in which the maximum value of θ_μ can be large enough to the taking place of EWB, when the cancellation happens between the contributions from θ_μ and θ_{A_0} to d_e . It results from that, the contributions from sleptons are highly suppressed by large slepton masses, in our chosen parameter space. It can be noted that, the contributions from θ_μ to d_e can be cancelled by θ_{M_2} , and θ_μ is the main source of baryon asymmetry, hence the worry about the contributions from the large value of θ_μ , which is needed to give rise to EWB, to the electron EDM whether can be cancelled is relaxed.

In the B-LSSM, there are new CPV phases $\theta_{\mu'}$, $\theta_{M_{BB'}}$ and $\theta_{M_{B'}}$ can make contributions to the electron EDM. In addition, the gaugino mass term M_1 can also have CPV phase θ_{M_1} , and makes contributions to d_e . Then we set other CPV phases equal to zero and explore the cancellation between $\theta_{\mu'}$, $\theta_{M_{BB'}}$, $\theta_{M_{B'}}$ and θ_{M_1} . Scanning the following regions of the parameter space:

$$\theta_{M_1} = (-\pi, \pi), \theta_{\mu'} = (-\pi, \pi), \theta_{M_{BB'}} = (-\pi, \pi), \theta_{M_{B'}} = (-\pi, \pi). \quad (17)$$

The allowed region of θ_{M_1} , $\theta_{M_{BB'}}$ is displayed in Fig. 6 (a), while the allowed region of θ_{M_1} , $\theta_{M_{B'}}$ is displayed in Fig. 6 (b). From the picture we can see that, when the possible

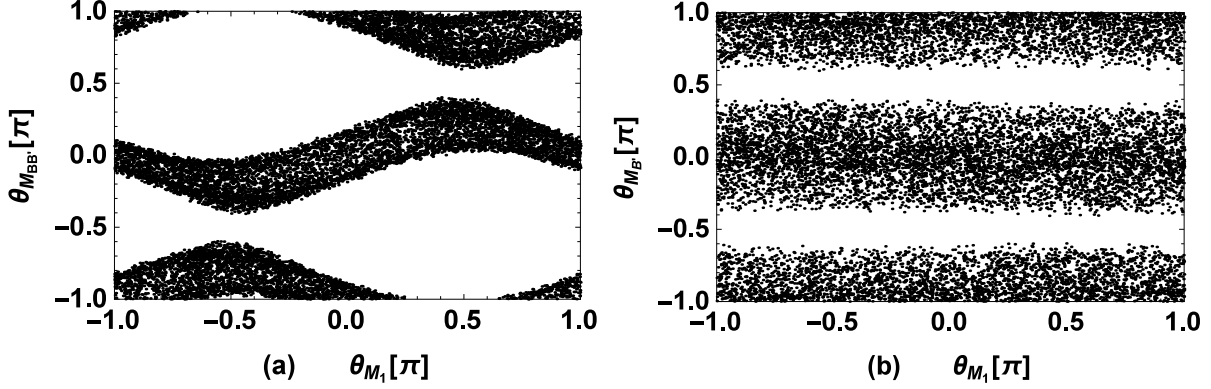


FIG. 6: Keeping $|d_e| < 8.7 \times 10^{-29}$, when the possible cancellation between θ_{M_1} , $\theta_{\mu'}$, $\theta_{M_{BB'}}$, $\theta_{M_{B'}}$ take place, the allowed regions of $\theta_{M_{BB'}}$, θ_{M_1} (a) and $\theta_{M_{B'}}$, θ_{M_1} (b) are plotted.

cancellation happens between θ_{M_1} and new phases $\theta_{\mu'}$, $\theta_{M_{BB'}}$, $\theta_{M_{B'}}$ in the B-LSSM, the constraint from d_e on θ_{M_1} can be relaxed completely. Comparing Fig. 6 (a) with Fig. 6 (b), it is obvious that the allowed region of θ_{M_1} versus $\theta_{M_{BB'}}$ as $\sin \theta_{M_{BB'}}$. But there is no obvious trend of the allowed region of θ_{M_1} with the changing of $\theta_{M_{B'}}$, which indicates that $\theta_{M_{BB'}}$ affects the numerical results more obviously than $\theta_{M_{B'}}$. Because $M_{BB'}$ is the mixing term between $\tilde{\lambda}_B$ and $\tilde{\lambda}_{B'}$, it contributes to d_e through the channel of $\tilde{\lambda}_B$ and $\tilde{\lambda}_{B'}$, when $M_{B'}$ contributes to d_e only through the channel of $\tilde{\lambda}_{B'}$.

Assuming all contributions from other phases are cancelled each other completely, and the only contribution to d_e comes from $\theta_{M_{BB'}}$. Then d_e versus $\theta_{M_{BB'}}$ is plotted in Fig. 7 (a), where the solid line, dashed line, dotted line denote $M_{BB'} = 0.1$ TeV, 0.14 TeV, 0.18 TeV respectively. Similarly, d_e versus $\theta_{M_{B'}}$ is plotted in Fig. 7 (b), where the solid line, dashed line, dotted line denote $M_{B'} = 0.6$ TeV, 0.9 TeV, 1.2 TeV respectively. The gray areas denote the present experimental upper bound on d_e . From the picture we can see that, $\theta_{M_{BB'}}$ or $\theta_{M_{B'}}$ affect the numerical results more obviously with the increasing of $M_{BB'}$ or $M_{B'}$, because the effects of $\theta_{M_{BB'}}$ or $\theta_{M_{B'}}$ are enlarged by large $M_{BB'}$ or $M_{B'}$. Comparing the effects of $M_{BB'}$ with $M_{B'}$, it can be noted that $M_{BB'}$ affect the numerical results more obviously than $M_{B'}$, which coincides with the discussion of Fig. 6 above.

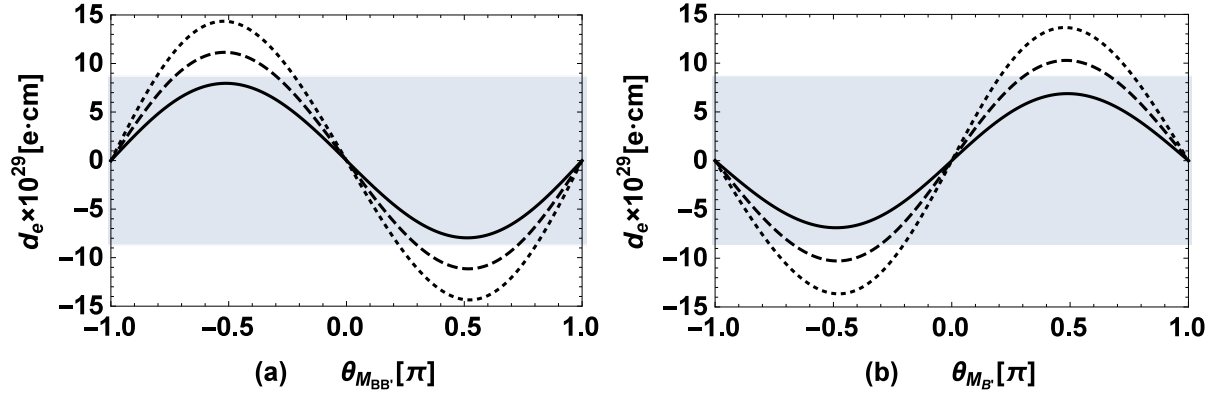


FIG. 7: d_e versus $\theta_{M_{BB'}}$ (a) for $M_{BB'} = 0.1$ TeV (solid line), 0.14 TeV (dashed line), 0.18 TeV (dotted line), and d_e versus $\theta_{M_{B'}}$ (b) for $M_{B'} = 0.6$ TeV (solid line), 0.9 TeV (dashed line), 1.2 TeV (dotted line), where the gray area denotes the present experimental upper bound on d_e .

V. SUMMARY

In this work, we focus on the CPV effects on EWB and electron EDM in the B-LSSM. Compared with the MSSM, new singlets mix with the MSSM doublets at the tree level, and a strong two-step PT can be achieved in this case. Moreover, new gaugino can make contributions to Y_B , and new coupling constant g_{Y_B} can affect the numerical results of Y_B obviously. When the resonant enhancement $\mu \approx M_{1,B'}$ or M_2 take place, the minimum value of θ_μ is about 0.03 to give rise to EWB. In this case, the contributions to the electron EDM must be enhanced vastly, the cancellation of the contributions from different CPV phases is needed. In addition, the main contributions to electron EDM come from charginos, and M_2 which also appears in the chargino sector can make comparable contributions with the μ term. Hence, the contributions from θ_μ to d_e can be cancelled by θ_{M_2} , and the worry about the contributions from the large value of θ_μ to the electron EDM whether can be cancelled is relaxed. In addition, new CPV phases $\theta_{\mu'}$, $\theta_{M_{BB'}}$, $\theta_{M_{B'}}$ in the B-LSSM also can cancel the contributions from θ_{M_1} to d_e , and the allowed region of θ_{M_1} is relaxed completely when the cancellation between θ_{M_1} and $\theta_{\mu'}$, $\theta_{M_{BB'}}$, $\theta_{M_{B'}}$ takes place. Assuming that the only contributions to d_e come from $M_{BB'}$ and $M_{B'}$, the numerical results show that, the experimental data of d_e favor $M_{BB'} \lesssim 0.1$ TeV, $M_{B'} \lesssim 0.6$ TeV when the regions of $\theta_{M_{BB'}}$

and $\theta_{M_{B'}}$ are relaxed completely.

Acknowledgments

The work has been supported by the National Natural Science Foundation of China (NNSFC) with Grants No. 11535002, and No. 11705045, Natural Science Foundation of Hebei province with Grants No. A2016201010, the youth top-notch talent support program of the Hebei Province, Hebei Key Lab of Optic-Eletronic Information and Materials, and the Midwest Universities Comprehensive Strength Promotion project.

-
- [1] R. Cooke, M. Pettini, R. A. Jorgenson, M. T. Murphy and C. C. Steidel, *Astrophys. J* **781**, 31 (2014).
 - [2] P. A. R. Ade *et al.* [Planck Collaboration], *Astron. Astrophys* **594**, A13 (2016).
 - [3] V. A. Kuzmin, V. A. Rubakov and M. E. Shaposhnikov, *Phys. Lett. B* **155**, 36 (1985).
 - [4] M. B. Gavela, A. Le Yaouanc, L. Oliver, O. Pene, J. C. Raynal and T. N. Pham, *Phys. Lett. B* **109**, 215 (1982).
 - [5] W. Bernreuther and M. Suzuki, *Rev. Mod. Phys* **63**, 313 (1991) Erratum: [*Rev. Mod. Phys* **64**, 633 (1992)].
 - [6] M. Pospelov and A. Ritz, *Phys. Rev. D* **89**, 056006 (2014).
 - [7] J. Baron et al, (ACME Collaboration), *Science* **343**, 269 (2014).
 - [8] M. Tanabashi et al, (Particle Data Group), *Phys. Rev. D* **98**, 030001 (2018).
 - [9] V. Andreev et al, (ACME Collaboration), *Nature* **562**, 355-360 (2018).
 - [10] M. Dine, P. Huet, R. L. Singleton, Jr and L. Susskind, *Phys. Lett. B* **257**, 351 (1991).
 - [11] A. G. Cohen and A. E. Nelson, *Phys. Lett. B* **297**, 111 (1992).
 - [12] P. Huet and A. E. Nelson, *Phys. Rev. D* **53**, 4578 (1996).
 - [13] D. Chang, W. F. Chang and W. Y. Keung, *Phys. Rev. D* **66**, 116008 (2002).
 - [14] C. Lee, V. Cirigliano and M. J. Ramsey-Musolf, *Phys. Rev. D* **71**, 075010 (2005).
 - [15] T. Konstandin, T. Prokopec, M. G. Schmidt and M. Seco, *Nucl. Phys. B* **738**, 1 (2006).

- [16] D. J. H. Chung, B. Garbrecht, M. J. Ramsey-Musolf and S. Tulin, Phys. Rev. Lett. **102**, 061301 (2009).
- [17] D. J. H. Chung, B. Garbrecht, M. J. Ramsey-Musolf and S. Tulin, JHEP **0912**, 067 (2009).
- [18] D. J. H. Chung, B. Garbrecht, M. J. Ramsey-Musolf and S. Tulin, Phys. Rev. D **81**, 063506 (2010).
- [19] V. Cirigliano, Y. Li, S. Profumo and M. J. Ramsey-Musolf, JHEP **1001**, 002 (2010).
- [20] C. W. Chiang and E. Senaha, JHEP **1006**, 030 (2010).
- [21] D. E. Morrissey and M. J. Ramsey-Musolf, New J. Phys. **14**, 125003 (2012).
- [22] J. Kozaczuk, S. Profumo, M. J. Ramsey-Musolf and C. L. Wainwright, Phys. Rev. D **86**, 096001 (2012).
- [23] M. Pietroni, Nucl. Phys. B **402**, 27 (1993).
- [24] A. T. Davies, C. D. Froggatt and R. G. Moorhouse, Phys. Lett. B **372**, 88 (1996).
- [25] S. J. Huber and M. G. Schmidt, Nucl. Phys. B **606**, 183 (2001).
- [26] J. Kang, P. Langacker, T. j. Li and T. Liu, Phys. Rev. Lett. **94**, 061801 (2005).
- [27] S. J. Huber, T. Konstandin, T. Prokopec and M. G. Schmidt, Nucl. Phys. B **757**, 172 (2006).
- [28] P. Nath, Phys. Rev. Lett **66**, 2565 (1991).
- [29] Y. Kizukuri and N. Oshimo, Phys. Rev. D **46**, 3025 (1992).
- [30] T. Falk and K. A. Olive, Phys. Lett. B **375**, 196 (1996).
- [31] T. Falk and K. A. Olive, Phys. Lett. B **439**, 71 (1998).
- [32] M. Brhlik, G. J. Good and G. L. Kane, Phys. Rev. D **59**, 115004 (1999).
- [33] A. Bartl, T. Gajdosik, W. Porod, P. Stockinger and H. Stremnitzer, Phys. Rev. D **60**, 073003 (1999).
- [34] S. Abel, S. Khalil and O. Lebedev, Nucl. Phys. B **606**, 151 (2001).
- [35] V. D. Barger, T. Falk, T. Han, J. Jiang, T. Li and T. Plehn, Phys. Rev. D **64**, 056007 (2001) [hep-ph/0101106].
- [36] K. A. Olive, M. Pospelov, A. Ritz and Y. Santoso, Phys. Rev. D **72**, 075001 (2005) [hep-ph/0506106].
- [37] V. Cirigliano, S. Profumo and M. J. Ramsey-Musolf, JHEP **0607**, 002 (2006) [hep-ph/0603246].

- [38] S. Yaser Ayazi and Y. Farzan, Phys. Rev. D **74**, 055008 (2006).
- [39] J. Engel, M. J. Ramsey-Musolf and U. van Kolck, Prog. Part. Nucl. Phys. **71**, 21 (2013).
- [40] T. Chupp, P. Fierlinger, M. Ramsey-Musolf and J. Singh, Rev. Mod. Phys. **91**, 015001 (2019).
- [41] V. Barger, P. Fileviez Perez and S. Spinner, Phys. Rev. Lett **102**, 181802 (2009).
- [42] P. Fileviez Perez and S. Spinner, Phys. Lett. B **673**, 251 (2009).
- [43] M. Ambroso and B. A. Ovrut, Int. J. Mod. Phys. A **26**, 1569 (2011).
- [44] P. F. Perez and S. Spinner, Phys. Rev. D **83**, 035004 (2011).
- [45] S. Khalil and H. Okada, Phys. Rev. D **79**, 083510 (2009).
- [46] L. Basso, B. OLeary, W. Porod and F. Staub, JHEP **1209**, 054 (2012).
- [47] L. Delle Rose, S. Khalil, S. J. D. King, C. Marzo, S. Moretti and C. S. Un, Phys. Rev. D **96**, 055004 (2017).
- [48] L. Delle Rose, S. Khalil, S. J. D. King, S. Kulkarni, C. Marzo, S. Moretti and C. S. Un, JHEP **1807**, 100 (2018).
- [49] W. Abdallah, A. Hammad, S. Khalil and S. Moretti, Phys. Rev. D **95**, 055019 (2017).
- [50] A. Elsayed, S. Khalil and S. Moretti, Phys. Lett. B **715**, 208 (2012).
- [51] G. Brooijmans et al. [arXiv:1203.1488 [hep-ph]].
- [52] L. Basso and F. Staub, Phys. Rev. D **87**, 015011 (2013).
- [53] L. Basso et al., Comput. Phys. Commun. **184**, 698 (2013).
- [54] A. Elsayed, S. Khalil, S. Moretti and A. Moursy, Phys. Rev. D **87**, 053010 (2013).
- [55] S. Khalil and S. Moretti, Rept. Prog. Phys **80**, 036201 (2017).
- [56] F. Staub, arXiv:0806.0538. F. Staub, Comput. Phys. Commun. **181** 1077-1086 (2010). F. Staub, Comput. Phys. Commun. **182** 808-833 (2011). F. Staub, Comput. Phys. Commun. **184** 1792-1809 (2013). F. Staub, Comput. Phys. Commun. **185** 1773-1790 (2014).
- [57] J. L. Yang, T. F. Feng, H. B. Zhang, G. Z. Ning and X. Y. Yang, Eur. Phys. J. C **78**, 438 (2018).
- [58] J. L. Yang, T. F. Feng, S. M. Zhao, R. F. Zhu, X. Y. Yang and H. B. Zhang, Eur. Phys. J. C **78**, 714 (2018).
- [59] J. L. Yang, T. F. Feng, Y. L. Yan, W. Li, S. M. Zhao and H. B. Zhang, Phys. Rev. D **99**, 015002 (2019).

- [60] D. Delepine, J. M. Gerard, R. Gonzalez Felipe and J. Weyers, Phys. Lett. B **386**, 183 (1996).
- [61] M. Carena, M. Quiros and C. E. M. Wagner, Phys. Lett. B **380**, 81 (1996).
- [62] J. R. Espinosa, Nucl. Phys. B **475**, 273 (1996).
- [63] M. Carena, M. Quiros and C. E. M. Wagner, Nucl. Phys. B **524**, 3 (1998).
- [64] S. J. Huber and M. G. Schmidt, Eur. Phys. J. C **10**, 473 (1999).
- [65] M. Carena, M. Quiros, M. Seco and C. E. M. Wagner, Nucl. Phys. B **650**, 24 (2003).
- [66] S. Profumo, M. J. Ramsey-Musolf and G. Shaughnessy, JHEP **0708**, 010 (2007).
- [67] M. Carena, G. Nardini, M. Quiros and C. E. M. Wagner, Nucl. Phys. B **812**, 243 (2009).
- [68] D. Curtin, P. Jaiswal and P. Meade, JHEP **1208**, 005 (2012).
- [69] K. Krizka, A. Kumar and D. E. Morrissey, Phys. Rev. D **87**, 095016 (2013).
- [70] H. H. Patel and M. J. Ramsey-Musolf, JHEP **1107**, 029 (2011).
- [71] H. B. Zhang, T. F. Feng, S. M. Zhao and T. J. Gao, Nucl. Phys. B **873**, 300 (2013) [Erratum: Nucl. Phys. B **879**, 235 (2014)].
- [72] H. B. Zhang, T. F. Feng, G. H. Luo, Z. F. Ge and S. M. Zhao, JHEP **1307**, 069 (2013) [Erratum: JHEP **1310**, 173 (2013)].
- [73] X. Y. Yang and T. F. Feng, Phys. Lett. B **675**, 43 (2009).
- [74] J. L. Yang, T. F. Feng, S. K. Cui, C. X. Liu, W. Li and H. B. Zhang, arXiv:1910.05868 [hep-ph].
- [75] M. Carena, J. R. Espinosa and C. E. M. Wagner, M. Quir, Phys. Lett. B **355**, 209 (1995).
- [76] M. Carena, M. Quiros and C. E. M. Wagner, Nucl. Phys. B, **461**, 407 (1996).
- [77] M. Carena, S. Gori, N.R. Shah and C. E. M. Wagner, JHEP, **03**, 014 (2012).
- [78] ATLAS Collab., ATLAS-CONF-2016-045.
- [79] G. Cacciapaglia, C. Csaki, G. Marandella, and A. Strumia, Phys.Rev. D **74**, 033011 (2006) [hep-ph/0604111] .
- [80] M. Carena, A. Daleo, B. A. Dobrescu and T. M. P. Tait, Phys. Rev. D **70**, 093009 (2004).
- [81] L. Alvarez-Gaume, J. Polchinski and M. B. Wise, Nucl. Phys. B **221**, 495 (1983).
- [82] A. Strumia, Nucl. Phys. B **482**, 24 (1996).
- [83] S. Profumo, M. J. Ramsey-Musolf and S. Tulin, Phys. Rev. D **75**, 075017 (2007).
- [84] J. M. Moreno, M. Quiros and M. Seco, Nucl. Phys. B **526**, 489 (1998).

- [85] P. John and M. G. Schmidt, Nucl. Phys. B **598**, 291 (2001) Erratum: [Nucl. Phys. B **648**, 449 (2003)].
- [86] S. Akula, C. Balzs, L. Dunn and G. White, JHEP **1711**, 051 (2017).
- [87] M. Carena, M. Quiros, A. Riotto, I. Vilja and C. E. M. Wagner, Nucl. Phys. B **503**, 387 (1997).
- [88] M. Carena, J. M. Moreno, M. Quiros, M. Seco and C. E. M. Wagner, Nucl. Phys. B **599**, 158 (2001).